Hill-Based Muscle Modeling

Ross H. Miller

Abstract

The Hill muscle model consists mainly of a contractile component (CC) in series with an elastic component (SEC) and is used widely in biomechanics and human movement science to actuate musculoskeletal models in simulations of human movement. This chapter summarizes the main features of Hill-based muscle models, including detailed treatments of the SEC force-extension relationship and the CC activation dynamics, force-length relationship, and force-velocity relationship. Additional model elements including CC pennation, parallel elasticity, history dependence, and metabolic energy expenditure are covered in brief. A contemporary summary of parameter values needed to implement muscle-specific models when creating models of the lower limb is included.

Keywords

Contractile component • Series elastic component • Activation • Force length • Force velocity • Parameters

Contents

R.H. Miller (✉)
Department of Kinesiology, University of Maryland, College Park, MD, USA
e-mail: rosshm@umd.edu

Introduction

Muscles are the motors of human motion: they receive input stimulation or "excitation" from the nervous system and in response produce force and perform work on the skeleton while consuming metabolic energy as fuel. The amount of force produced depends heavily on three factors: the magnitude and timing of excitation, the kinematic state of the muscle, and the morphological/physiological properties of the muscle. These factors can be well represented by a simple mechanical model known as the Hill muscle model (Fig. 1), consisting principally of a contractile component (CC) in series with an elastic component (SEC). Due to this simplicity and the consequent ease of implementation on computers, Hill-based muscle models are by far the most commonly used actuator in computer models of human movement (chapter ▶ "Optimal Control Modeling of Human Movement"). This chapter provides an overview of creating and using Hill-based muscle models. A summary of muscle-specific parameter values seen in the literature is included.

Muscle models other than Hill-based models are not included in this chapter due to their infrequent use in human motion analysis and their poor performance during lengthening contractions (Cole et al. 1996). For details on the other major class of muscle models in biomechanics, Huxley-based models, readers are referred to Huxley (1957), Hill (1974), Zahalak (1981), and Cole et al. (1996).

State of the Art

The origin of the Hill model dates to the work of A.V. Hill (1886–1977), who won the 1922 Nobel Prize in Physiology or Medicine for his work relating the mechanics and energetics of force production in the skeletal muscle. Hill himself was not a computer modeler, nor did he name the model after himself, but he conceived of the model depicted in Fig. 1a to explain his observations on the force produced in vitro
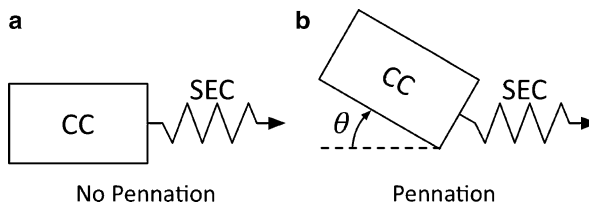
Fig. 1 (**a**) The two-component Hill muscle model with a contractile component (CC) in series with an elastic component (SEC). (**b**) The model including the CC pennation angle θ

by frog sartorius at different shortening velocities (Hill 1938). The earliest efforts at formal computational simulations using a model based on Hill's work were made by Bahler (1968) for an isolated muscle and by Hatze (1976) in simulations of whole-body human movement. Additional features on top of basic two-component model shown in Fig. 1a include parallel elastic components representing the passive stiffness of inactive muscle (e.g., Siebert et al. 2008), pennation of the CC representing muscle fiber orientation (e.g., van den Bogert et al. 2011), models that consider muscle fiber-type histology (e.g., Lee et al. 2013), and models of muscle energy expenditure (e.g., Umberger et al. 2003). However, the central aspect of modeling muscle as a set of differential equations representing the activation and contractile dynamics of force production has been essentially unchanged since the 1960s.

The reader should be mindful that the Hill model is a *phenomenological model*. Its purpose is to accurately simulate muscle force production for a variety of input excitation conditions and *whole-muscle* (origin-to-insertion) kinematic states. The CC and SEC in the Hill model capture many of the aspects of muscle force production typically attributed to fibers and tendons respectively in real muscle, but the CC and SEC do not have direct anatomical analogues in real muscle. Hill himself cautioned against an anatomical interpretation of the model's components:

> For simplicity in description the [SEC] will be referred to as "tendon", but no assumption is implied that other undamped series elastic elements do not exist within the fibers themselves; the evidence of its properties is derived from mechanical experiments with active muscle, not from histological observation. (Hill 1950)

This caution has implications in how Hill-based models are parameterized and in the interpretation and validation of their output vs. measurements from real muscle. The interested reader is also referred to the recent review on verification and validation of musculoskeletal models by Hicks et al. (2015).

Hill Muscle Model Formalisms

The core components of a Hill-based muscle model are the CC and the SEC (Fig. 1). The CC represents aspects of muscle that actively produce force in response to excitation. This force is expressed across the SEC, which responds elastically. The equations of kinematic and kinetic equilibrium are:

$$L_m = L_{CC} + L_{SEC} \tag{1}$$

$$F_{CC} = F_{SEC} \tag{2}$$

where L_m is the muscle origin-to-insertion length, L_{CC} and L_{SEC} are the CC and SEC lengths, and F_{CC} and F_{SEC} are the CC and SEC forces. Introducing the pennation angle θ from Fig. 1b:

$$L_m = L_{CC} \cos \theta + L_{SEC} \tag{3}$$

$$F_{CC} \cos \theta = F_{SEC} \tag{4}$$

Pennation is typically implemented by assuming the CC has constant volume and constant thickness:

$$L_{CC} \sin \theta = L_o \sin \theta_o \tag{5}$$

where L_o is the optimal CC length in the sense of the force-length relationship (Gordon et al. 1966) and θ_o is the pennation angle when $L_{CC} = L_o$.

The Series Elastic Component

The SEC in the Hill model behaves elastically according to a force-extension relationship, where the SEC force is zero below its unloaded length L_u and increases to progressively greater force when stretched to progressively longer lengths beyond L_u. Measurements of SEC force and extension suggest their relationship is nonlinear (Hill 1950). A common nonlinear model assumes the force-extension relationship is quadratic (van Soest and Bobbert 1993):

$$F_{SEC} = \begin{cases} K_1(L_{SEC} - L_u)^2, & L_{SEC} > L_u \\ 0, & L_{SEC} \leq L_u \end{cases} \tag{6}$$

$$K_1 = F_o/(U_o L_u)^2 \tag{7}$$

where F_o is the maximum isometric force and U_o is the SEC strain when it is loaded with the maximum isometric force (i.e., when $F_{SEC} = F_o$). Typical values for U_o based on tendon measurements or quick-release experiments are 0.03–0.10. A constant value of $U_o = 0.04$ is often assumed for all muscles, although this assumption appears to be based more on tradition following the original source (van Soest and Bobbert 1993) rather than evidence that U_o is indeed invariant between muscles and subjects. The choice of U_o dictates the stiffness of the SEC, which has a major effect on muscle energetics (Lichtwark and Wilson 2007).

When using gradient-based simulation methods, it is often desirable for the model's state equations to have nonzero gradients. Equation 6 can be modified to meet this condition by adding a linear term:

$$F_{SEC} = K_0(L_{SEC} - L_u) + \begin{cases} K_1(L_{SEC} - L_u)^2, & L_{SEC} > L_u \\ 0, & L_{SEC} \leq L_u \end{cases} \tag{8}$$

where K_0 has a small nonzero value (e.g., 1–10 N/m). Alternatively, the force-extension relationship has been modeled as exponential (Caldwell 1995):

$$F_{SEC} = F_o C_o(\exp(K_2(L_{SEC}/L_u - 1)) - 1) \tag{9}$$

where C_o and K_2 are constants used to fit the curve to measurements. Values of $C_o = 0.0258$ and $K_2 = 92.08$ give a curve with about 4% extension when $F_{SEC} = F_o$, although the shape of this force-extension curve differs substantially from the shape of Eq. 8 with $U_o = 0.04$ (Fig. 2).

The SEC is by definition undamped (Hill 1938, 1950), but a small amount of damping can improve the numerical efficiency and stability of the model (Günther et al. 2007) and is motivated physiologically by the water content of connective tissue. A specific example of implementing SEC damping is a linear parallel damper:

$$F_{SEC} = K_1 (L_{SEC} - L_u)^2 + D_{SEC} \dot{L}_{SEC} \qquad (10)$$

where $\boldsymbol{D_{SEC}}$ is the damping rate. Interested readers are referred to Günther et al. (2007).

The Contractile Component

Activation dynamics. The Hill model receives as input a time-varying neural excitation signal $\boldsymbol{u}(t)$ that represents the summed motor unit action potentials and ranges on [0,1]. In response to this signal, the CC activates its "contractile machinery" represented by the activation level α, a nondimensional parameter that also ranges on [0,1] depending on the history of excitation. Under the crossbridge theory of muscle force production (Huxley 1957), α is analogous to the fraction of binding sites on actin unblocked by troponin and available for crossbridge formation. The chemical reactions responsible for the rise and fall of activation in response to changes in excitation occur over finite time periods. Activation therefore lags behind the time course of excitation. He et al. (1991) presented a model of these activation dynamics
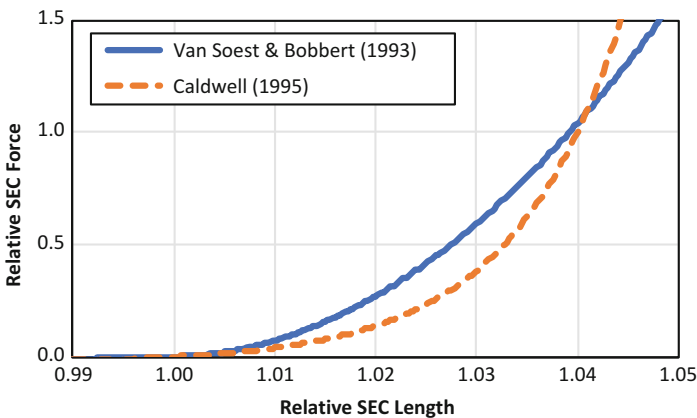
Fig. 2 Force-extension relationships of the SEC as defined by van Soest and Bobbert (1993) and Caldwell (1995). SEC length is relative to the unloaded length. SEC force is relative to the maximum isometric force

that has been used in many studies and captures the observation that activation rises faster than it falls:

$$\dot{\alpha} = (u - \alpha)(c_1 u + c_2) \tag{11}$$

$$c_2 = 1/\tau_2 \tag{12}$$

$$c_1 = 1/\tau_1 - c_2 \tag{13}$$

where τ_1 and τ_2 are time constants for rising and falling activation, respectively. Typical time constants are on the order of 10–100 ms and are affected by muscle fiber type. Umberger et al. (2003) modeled the time constants as:

$$\tau_1 = 0.080 - 0.050FT \tag{14}$$

$$\tau_2 = 0.095 - 0.060FT \tag{15}$$

where FT is the fraction of fast-twitch fibers in the muscle. The sensitivity of activation to FT during a burst of maximum excitation is demonstrated in Fig. 3.

More complicated models of neuromuscular control exist, but their details are excluded here for brevity and to maintain the focus on muscle modeling. For example, Hatze (1976, 1977) defined two control signals per muscle representing motor unit recruitment and rate-coding separately; Fuglevand et al. (1993) developed a detailed model of motor neurons, motor unit pools, and surface electromyograms; and Buchanan et al. (2004) presented a comprehensive summary of methods for using raw electromyogram measurements as the control input to Hill-based muscle models. Interested readers are referred to those references for details.
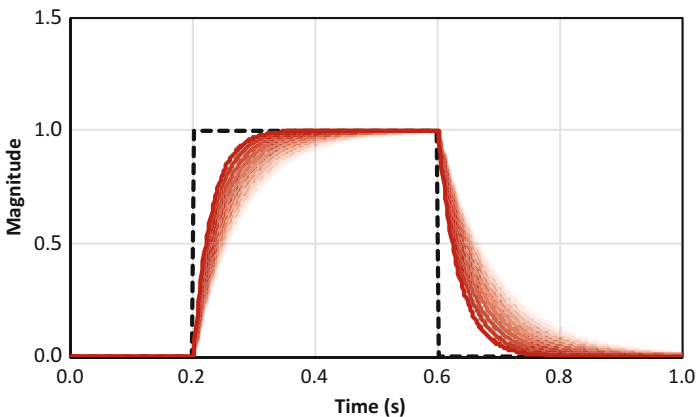
Fig. 3 Muscle excitation (*dashed line*) and activation from the He et al. (1991) model (*solid lines*) during a 400 ms burst of maximal excitation preceded and followed by zero excitation. Progressively darker shades of activation are progressively greater values of FT from 0.0 to 1.0

Force. The CC force is typically modeled as a function of its instantaneous activation and kinematic state:

$$F_{CC} = f_{CC}(\alpha, L_{CC}, \dot{L}_{CC}) \tag{16}$$

The specific form of the function f_{CC} has varied between studies. A common assumption is that the effects of the three input arguments are multiplicative and independent:

$$F_{CC} = F_o \cdot \alpha \cdot FL \cdot FV \tag{17}$$

where FL and FV are nondimensional factors representing the influence of the force-length and force-velocity relationships, described below.

Force-length relationship. It is well known that the amount of force the CC can produce depends on its current length (Gordon et al. 1966). The CC can produce the most force at a moderate length defined as its optimal length L_o, with progressively less force production possible at progressively longer or shorter lengths. The force-length relationship is often modeled as parabolic (Woittiez et al. 1983):

$$FL = \max\left(-\frac{1}{W_1^2}\left(\frac{L_{CC}}{L_o} - 1\right)^2 + 1, 0\right) \tag{18}$$

where W_1 is the width of the force-length parabola in multiples of L_o. A form of the force-length relationship better suited for gradient-based simulation methods is the Gaussian force-length relationship (Winters and Stark 1985):

$$FL = \exp\left(-\frac{1}{W_2}\left(\frac{L_{CC}}{L_o} - 1\right)^2\right) \tag{19}$$

where W_2 affects the width of the curve but does not directly define its zero-crossings. The parabolic and Gaussian curves are compared in Fig. 4a. Hatze (1977) proposed a more complicated force-length relationship:

$$FL = 0.32 + 0.71\exp\left(-1.112\left(\frac{L_{CC}}{L_o} - 1\right)\right) \sin\left(3.722\left(\frac{L_{CC}}{L_o} - 0.656\right)\right) \tag{20}$$

where the constants were derived to fit the curve to sarcomere force-length data from Gordon et al. (1966) over the interval $L_{CC}/L_o \in [0.58, 1.80]$. Whole-muscle force-length curves are often much wider than sarcomere force-length curves (van den Bogert et al. 1998), so Eqs. 18 and 19 are recommended for musculoskeletal modeling.

In real muscle the optimal CC length L_o is not constant but rather shortens as the activation level α increases (Huijing 1996). This effect can be included in the Hill model with a simple linear relationship:
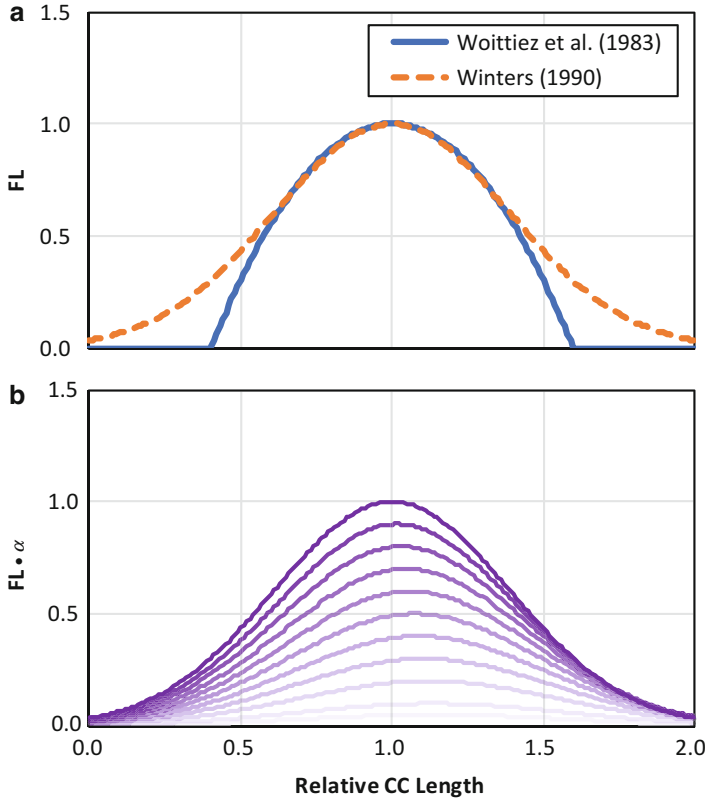
Fig. 4 (**a**) Force-length relationships for a parabolic curve (Woittiez et al. 1983) and a Gaussian curve (Winters and Stark 1985). The parameter values were $W_1 = 0.60$ and $W_2 = 0.30$. CC length is relative to CC optimal length. (**b**) The Gaussian force-length relationship with an activation-dependent optimal length (Lloyd and Besier 2003). Progressively darker shades are progressively greater activations from 0.05 to 1.00

$$L_o = L_\alpha(\gamma(1 - \alpha) + 1) \tag{21}$$

where L_α is the optimal CC length at maximum activation. A typical value for the constant γ is 0.15 (Lloyd and Besier 2003). Figure 4b demonstrates the sensitivity of the force-length relationship's shape to activation level when the optimal length is modeled as activation dependent using Eq. 21.

Force-velocity relationship. The force-velocity relationship is perhaps the most well-known mechanical property of skeletal muscle. McLean et al. (2003) presented a nondimensional relationship that captures the main features of both the concentric and eccentric limbs of the force-velocity relationship (Hill 1938; Katz 1939):

$$FV = \begin{cases} \dfrac{b + a\dot{L}_{CC}/L_o}{b - \dot{L}_{CC}/L_o}, & \dot{L}_{CC}/L_o \leq 0 \\[2ex] \dfrac{C_{ecc}\dot{L}_{CC}/L_o + v_1}{\dot{L}_{CC}/L_o + v_1}, & 0 < \dot{L}_{CC}/L_o \leq \delta v_1 \\[2ex] v_3 + v_2\dot{L}_{CC}/L_o, & \dot{L}_{CC}/L_o > \delta v_1 \end{cases} \tag{22}$$

$$v_1 = \frac{(C_{ecc} - 1)b}{a + 1} \tag{23}$$

$$v_2 = \frac{a + 1}{b(\delta + 1)^2} \tag{24}$$

$$v_3 = \frac{(C_{ecc} - 1)\delta^2}{(\delta + 1)^2} + 1 \tag{25}$$

The parameters a and b are constants, and their ratio b/a defines the CC maximum shortening velocity v_{max}. Umberger et al. (2003) defined their values as functions of fiber type, such that muscles with greater fast-twitch fiber fractions can produce more force at a given velocity of shortening (Fig. 5c):

$$a = 0.1 + 0.4FT \tag{26}$$

$$b = v_{max}a \tag{27}$$

The parameter C_{ecc} is the eccentric asymptote for force during lengthening, such that the CC force asymptotically approaches $C_{ecc}F_o$ as the velocity of lengthening increases. Typical parameter values are $C_{ecc} = 1.3–1.8$ and $v_{max} = 9–13$. Equation 25 replaces the hyperbolic eccentric force-velocity curve with a linear curve during "fast" lengthening, which can be necessary for some implementations of Eq. 22 on computers. The parameter δ defines the threshold between "slow" and "fast" lengthening and has a suggested value of 5.67 (McLean et al. 2003).

The maximum shortening velocity v_{max} in real muscle increases with increasing activation level α (Chow and Darling 1999). The dependency can be included in the Hill model by multiplying the value of b during shortening contractions (Eq. 22) by an activation-dependent scaling factor λ. McLean et al. (2003) suggested the following factor to fit the Chow and Darling (1999) data:

$$\lambda = 1 - \exp(-3.82\alpha) + \alpha \exp(-3.82) \tag{28}$$

Umberger et al. (2003) suggested a simpler factor:

$$\lambda = \alpha^{-0.3} \tag{29}$$

Note that these factors scale b during shortening contractions only; the maximum value of b (Eq. 27) is used during lengthening. Figure 5b demonstrates the sensitivity

Fig. 5 (**a**) Force-velocity
relationships from McLean
et al. (2003) and Hatze (1977).
The parameter values were
$C_{ecc} = 1.45$, $FT = 0.50$,
$v_{max} = 12$, $A_H = 2.64$, and
$B_H = -0.137$. CC velocity
is relative to CC optimal
length. (**b**) Effect of activation
level on the shape of the
McLean et al. (2003) force-
velocity curve. Progressively
darker shades are
progressively greater
activations from 0.05 to 1.00.
(**c**) Effect of fiber type on the
shape of the McLean et al.
(2003) force-velocity curve.
Progressively darker shades
are progressively greater
values of FT from 0.0 to 1.0
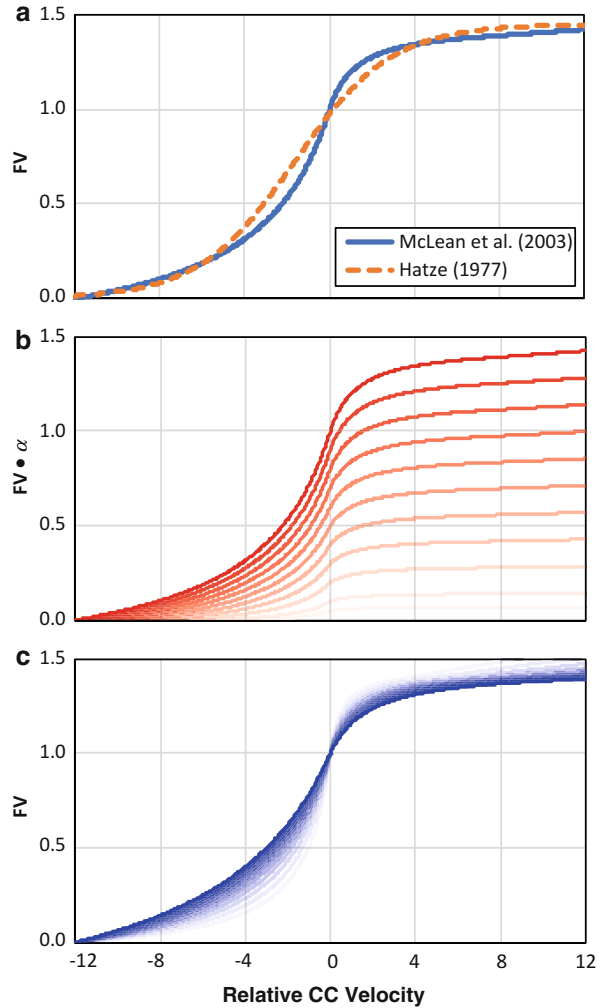
of the McLean et al. (2003) force-velocity curve to activation-dependent scaling of
v_{max} using Eq. 29.

Numerous other forms of the force-velocity relationship conceptually similar to
Eq. 25 have been presented (e.g., van Soest and Bobbert 1993; Minetti and Alex-
ander 1997). Hatze (1977) alternatively defined the force-velocity relationship as a
single function for both shortening and lengthening velocities:

$$FV = \frac{C_{ecc}}{2}\left(1 + \tanh\left(A_H\left(\frac{\dot{L}_{CC}}{v_{max}L_o} - B_H\right)\right)\right) \tag{30}$$

The advantage of Eq. 30 over Eq. 22 is that it does not require logical statements to implement in code and thus avoids any potential discontinuities at zero velocity. The disadvantages are that including dependencies on activation and fiber type is more challenging, FV is not exactly 1.0 at $\dot{L}_{CC} = 0$, and the constants $\boldsymbol{A_H}$ and $\boldsymbol{B_H}$ have no direct relationship to the Hill constants a and b. Typical values are $A_H = 3.0$ and $B_H = -0.10$. Figure 5a compares the shapes of the McLean et al. (2003) and Hatze (1977) force-length relationships, with rather substantial differences at moderate velocities.

Additional Features

Most Hill muscle models include the basic elements described already: an SEC with a force-extension relationship and a CC with activation dynamics and force-length-velocity relationships. Additional features in some models include a parallel elastic component, history-dependent force production, and metabolic energy expenditure.

Parallel elasticity. The CC by definition is the source of the muscle's "active" force, i.e., the force produced by activation of the muscle's contractile machinery in response to excitation from the nervous system. The "passive" force of the muscle is then the force due to muscle's material properties in the absence of activation (Gordon et al. 1966). The distinction between active and passive force has blurred recently with the emergence of titin as a potential third contractile protein. However, many Hill-based models include a third component along with the CC and SEC in the form of a parallel elastic component (PEC). The PEC is included either parallel to the whole muscle or parallel to the CC only (Fig. 6) and produces a force $\boldsymbol{F_{PEC}}$ as a function of its length $\boldsymbol{L_{PEC}}$ using a function similar to the SEC force-extension relationship. When placed in parallel with the CC only, the PEC force is a function of CC length and Eq. 4 becomes:

$$(F_{CC} + F_{PEC}) \cos\theta = F_{SEC} \tag{31}$$
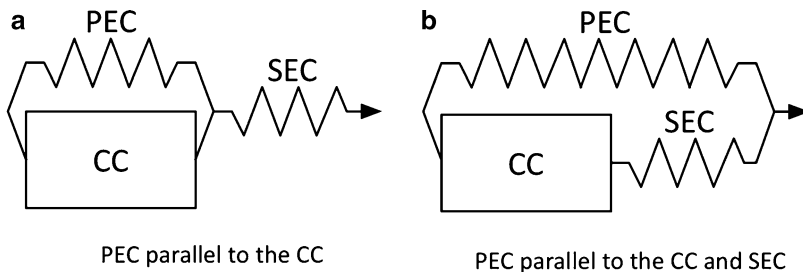
Fig. 6 Three-component Hill muscle model with a parallel elastic component (PEC) situated (**a**) parallel to only the CC and (**b**) parallel to both the CC and the SEC

When placed in parallel with the whole muscle, the PEC force is a function of whole-muscle length, and a new variable representing the whole-muscle force F_m must be defined:

$$F_m = F_{PEC} + F_{SEC} = F_{PEC} + F_{CC} \cos \theta \tag{32}$$

Equation 31 typically produces slightly better agreement with force measurements from real muscle (e.g., Siebert et al. 2008), while Eq. 32 is advantageous because it can be implemented in musculoskeletal models at the joint level (e.g., Riener and Edrich 1999) and avoids the need to model parallel elasticity at the individual muscle level.

History dependence. In the Hill models described so far, the force produced by the CC depends only on its current kinematic state. It has long been known that CC force also depends on the recent history of its length, i.e., history-dependent force enhancement and force depression (Abbott and Aubert 1952). Briefly:

- When a muscle is stretched then shortened to and held at a particular length, it produces more force than would be produced by an isometric contraction at that same length (force enhancement).
- When a muscle is shortened then stretched to and held at a particular length, it produces less force than would be produced by an isometric contraction at that same length (force depression).

Both effects have been observed in human muscles in vivo under voluntary sub-maximal contractions, suggesting they should be included in models of human movement (Herzog 2004). Readers interested in implementing history-dependent phenomena in a Hill-based model are referred to the relatively simple model by Forcinito et al. (1998) and the more complex model by McGowan et al. (2013).

Metabolic energy expenditure. Skeletal muscles produce force and perform work on the skeleton, at the cost of consuming metabolic energy. The rate at which energy is consumed appears to be a critical factor in human motor behavior (e.g., Srinivasan 2009), and there has been considerable interest in including models of muscle energy expenditure in Hill-based muscle models such that whole-body energy expenditure can be accounted for in simulations of movement (e.g., Miller 2014). A simple model of muscle energy expenditure was proposed by Minetti and Alexander (1997):

$$\dot{E} = \alpha F_o L_o v_{max} \left(\frac{0.054 + 0.0506 v_{CC} + 2.46 v_{CC}^2}{1 - 1.13 v_{CC} + 12.8 v_{CC}^2 - 1.64 v_{CC}^3} \right) \tag{33}$$

$$v_{CC} = \dot{L}_{CC} / v_{max} \tag{34}$$

where $\dot{E}$ is the muscle's rate of metabolic energy expenditure (per unit time) and the constants were determined from curve-fitting to measured data from frog muscle. This model assumes that energy expenditure is affected only by activation and CC velocity, but it does not appear to produce inferior results to other more detailed

models (Miller 2014). Other models are based primarily on the first law of thermo-dynamics (e.g., Umberger et al. 2003):

$$\dot{E} = \dot{H} - \dot{F}_{CC}\dot{L}_{CC} \tag{35}$$

where $\dot{H}$ is the rate of heat liberation, which generally depends on activation and the CC kinematic state, and $\dot{F}_{CC}\dot{L}_{CC}$ is the CC mechanical work rate, assuming shortening velocities are negative. A difficulty with these types of models is the need to account for the energetic fate of eccentric muscle work, which is not well understood.

Muscle-Skeleton Kinematic Coupling

Muscles attach to at least two different bones, implying that their origin-to-insertion length (L_m in Eq. 1) is a function of the skeletal pose $\mathbf{q}$. The approach to modeling kinematic coupling will determine the relationship between the skeletal pose and moment arms of a muscle's force to the rotational centers of the skeleton's joints and will have an indirect effect on muscle force production through Eq. 1 (chapter ▶ "Three-Dimensional Reconstruction of the Human Skeleton in Motion").

The two common approaches for modeling muscle-skeleton kinematic coupling are the geometric approach and the curve-fitting approach. With the geometric approach, each muscle is represented as a set of n coordinate points in local skeletal segment reference frames (e.g., Delp et al. 1990). To determine the muscle's length and moment arm, consider a muscle with its origin on segment A and its insertion on segment B, defined by n coordinate points. Points $\mathbf{p}_1$ through $\mathbf{p}_{m-1}$ are defined in reference frame A, and points $\mathbf{p}_m$ through $\mathbf{p}_n$ are defined in reference frame $\mathbf{B}$. The length of the muscle in a given skeletal pose is the sum of the distances between each consecutive pair of coordinates:

$$L_m = \sum_{i=1}^{n-1} \left| \mathbf{p}_{i+1} - \mathbf{p}_i \right| \tag{36}$$

The muscle's moment arm $\mathbf{r}$ with respect to a generalized coordinate q that defines the pose of B relative to A can be determined directly from the coordinate points using the partial velocity method:

$$r = \left(\frac{\partial \mathbf{f}_r(\mathbf{q})}{\partial q} \times \mathbf{p}_m^A + \frac{\partial \mathbf{f}_t(\mathbf{q})}{\partial q} \right) \cdot (\mathbf{p}_m - \mathbf{p}_{m-1}) \tag{37}$$

where $\mathbf{f}_r(\mathbf{q})$ and $\mathbf{f}_t(\mathbf{q})$ are the functions defining the respective rotations and translations between the two reference frames and $\mathbf{p}_m^A$ is the position of point $\mathbf{p}_m$ in reference frame $\mathbf{A}$.

With the curve-fitting approach, models like Delp et al. (1990), cadaver experiments, or in vivo imaging are used to obtain data for muscle lengths at different joint angles (chapters ▶ "Ultrasound Technology for Examining the Mechanics of the Muscle, Tendon, and Ligament" and ▶ "3D Musculoskeletal Kinematics Using Dynamic MRI"). These data are then fit with a differentiable polynomial function $L_m(\mathbf{q})$:

$$L_m(\mathbf{q}) = \sum_{i=1}^{N} a_i \prod_{j=1}^{M} q_j^{p_{ij}} \tag{38}$$

where N is the number of polynomial terms, $\boldsymbol{a_i}$ are the polynomial coefficients, $\boldsymbol{M}$ is the number of generalized coordinates actuated by the muscle, and $\boldsymbol{p_{ij}}$ are the polynomial exponents. Moment arm functions can be derived analytically using the virtual work method:

$$r(\mathbf{q}) = -\frac{\partial L_m(\mathbf{q})}{\partial q_j} \tag{39}$$

In some cases, first-degree polynomials equating to the assumption of constant moment arm lengths may be sufficient (e.g., sagittal plane models simulating small ranges of joint motion).

Equation 37 is also technically the partial derivative of muscle length with respect to q; the curve-fitting method can be considered an approximation of the geometric method. The choice of the fitting function for Eq. 38 will depend on the desired level of accuracy with the data source and will influence the moment arms obtained and the muscle forces and joint moments produced. The curve-fitting approach produces equations that are more convenient for simulation methods involving symbolic gradients (e.g., van den Bogert et al. 2011). Defining subject-specific coupling parameters requires the same data with both approaches. Geometric scaling based on body or segment dimensions is more straightforward with the geometric approach. Regardless of the approach chosen, it is relevant to consider that some muscle moment arms depend not only on skeletal pose but also on muscle force (e.g., Maganaris et al. 1998). Readers interested in more comprehensive treatments of kinematic modeling of muscles are referred to An et al. (1984), Zajac and Gordon (1989), and Pandy (1999).

Implementation

Hill-based models are often implemented in simulations of human movement by defining the activation $\boldsymbol{\alpha}$ and the CC length $\boldsymbol{L_{CC}}$ as state variables. The model's state equations are then a set of two first-order ordinary differential equations, one

describing the activation dynamics and one describing the contractile dynamics. An example algorithm for implementing a Hill-based model in a forward dynamics application is:

1. Receive initial values for α and L_{CC} and current values for u and L_m
2. Knowing α and u, calculate $\dot{\alpha}$ from the activation dynamics
3. Knowing L_{CC} and L_m, calculate L_{SEC} from kinematic equilibrium
4. Knowing L_{SEC}, calculate F_{SEC} from the SEC force-extension relationship
5. Knowing F_{SEC}, calculate F_{CC} from kinetic equilibrium
6. Knowing F_{CC}, α, and L_{CC}, calculate $\dot{L}_{CC}$ from the CC force definition
7. Use $\dot{\alpha}$ and $\dot{L}_{CC}$ to update α and L_{CC} for the next timestep by numerical integration
8. Iterate until the final time is reached

Steps 2 and 6 can be completed using basic algebra for the simplest Hill models. More complicated models may require analytical or numerical root-finding methods. Methods of numerical integration in Step 7 are outside the scope of this chapter, but methods with greater accuracy than the basic Euler method are typically required.

The series of steps above is a traditional "forward dynamics" simulation method: starting from a known initial state, the model's dynamics are used to integrate the state forward in time to calculate future states at other timesteps. Some alternative methods of simulation involve knowledge of the state variables at all timesteps, in which case the muscle model dynamics are implemented as constraints on the feasible solution domain. For example, with implicit direct collocation (van den Bogert et al. 2011), the muscle model is a set of equality constraints:

$$\dot{\alpha} - (u - \alpha)(c_1 u + c_2) = 0 \qquad (40)$$

$$f_{SEC}(L_{SEC}) - f_{CC}(\alpha, L_{CC}, \dot{L}_{CC}) = 0 \qquad (41)$$

where $\dot{\alpha}$ and $\dot{L}_{CC}$ are estimated by finite differences (chapter ▶ "Optimal Control Modeling of Human Movement").

Hill Model Parameters

Hill-based muscle models have a substantial number of parameters that must be specified before numerical simulations can be performed in practice. Even models consisting of only the most basic elements with the simplest formulations described in this chapter require at least eight independent parameter values per muscle. When simulating the actions of a specific muscle or a whole-body motion actuated by many muscles, it is important for these parameter values to be defined on an appropriate muscle-specific basis and perhaps on a subject-specific basis depending on the use of the model. The process of assigning many parameters for many muscle models can be daunting, especially for new users who may be unfamiliar with the necessity and

rationale, available resources, and methods for doing so. Here a current summary is presented for parameter values in the muscle literature useful for Hill-based muscle modeling. The five parameters considered were:

1. Optimal fiber length (L_o)
2. Fiber pennation angle (θ)
3. Physiological cross-sectional area (PCSA)
4. Unloaded tendon length (L_u)
5. The fraction of "fast-twitch" fibers (FT)

The first four parameters were selected due to the volume of available data and the high sensitivity of Hill model output to their values (e.g., Scovil and Ronsky 2006). Data on FT were included due to their importance in some models of muscle energy expenditure (e.g., Umberger et al. 2003).

Readers should be aware that most of the parameter values presented here are derived from measurements on real muscle fibers and tendons, which are not the anatomical analogs of the Hill model CC and SEC. The values given here can provide a starting point for selecting parameter values in muscle models, but they may not be the final values needed to produce good results in a particular use case. For example, synergy between the parameters relating to contractile dynamics and those relating to muscle-skeleton kinematic coupling needs to be considered.

Optimal fiber length. Methods of determining L_o from muscle fiber measurements have varied in the literature. Some studies have determined fiber length from manual ruler-based measurements. In these cases, it is often the fascicle length (not the fiber length) that is actually measured, with the assumption that the fibers run the full length of the fascicles. This assumption is controversial particularly for long fascicles (Trotter 1990). Another common method of determining L_o has been to report fiber lengths that have been "normalized" using sarcomere length measurements:

$$L_{Fn} = L_{Fm}L_{So}/L_{Sm} \tag{42}$$

where $\boldsymbol{L_{Fn}}$ is the normalized fiber length, $\boldsymbol{L_{Fm}}$ is the originally measured fiber length, $\boldsymbol{L_{So}}$ is the optimal sarcomere length in the context of the sliding filament hypothesis and the force-length relationship, and $\boldsymbol{L_{Sm}}$ is the measured sarcomere length. The purpose of normalization is to obtain an estimate of optimal fiber length L_o, i.e., $L_{Fn} \approx L_o$. The obvious challenge in normalization is that measurements of sarcomere length are required. The optimal sarcomere length for human muscle appears to be about 2.6–2.8 μm (Walker and Schroedt 1974; Lieber et al. 1994). Unless otherwise noted, all fiber lengths that were normalized to an optimal sarcomere length other than 2.7 μm in the referenced data were renormalized to an optimal length of 2.7 μm for presentation here.

Another method for determining L_o has been to use muscle modeling and optimization to adjust the value of L_o (and various other model parameters) to track measurements of human joint torque production as possible (Hatze 1981; Hasson and Caldwell 2012). This allows for in vivo determination of L_o (and various

other model parameters) without medical imaging equipment and is also faithful to the phenomenological "input/output" nature of the Hill model.

Fiber pennation angle. Fiber pennation angle $\boldsymbol{\theta}$ is typically defined as the orientation of the long axis of the muscle fibers or fascicles, relative to the tendon. This definition has been used fairly consistently in the literature. Cadaver studies by necessity measure θ when muscles are inactive. In vivo studies have sometimes measured θ at rest or during active contractions and at various joint angles. These factors should be considered when interpreting in vivo θ data because fiber length and activation level will affect the current θ.

Most studies have measured θ from a single plane and report a representative or average result for the muscle in question. This definition of θ is likely not reflective of the full fiber geometry in a three-dimensional muscle, but it is consistent with how θ is usually included in Hill-based models, where constant muscle thickness and volume are assumed. Infrequently, more detailed multi-planar definitions of θ have been used, and occasionally the distribution of pennation angles within the fibers of the muscle has been assessed (e.g., Scott et al. 1993).

Physiological cross-sectional area. PCSA has been defined inconsistently in the literature. Some studies use the definition of Alexander and Vernon (1975):

$$PCSA_1 = V/L_o \qquad (43)$$

where V is the total volume of fibers within the muscle. This definition is advantageous because it has an intuitive geometrical interpretation (the cross-sectional area of contractile material perpendicular to the long axis of the muscle fibers) and because the product with the specific tension σ gives the maximum isometric force of the CC:

$$F_o = PCSA_1 \cdot \sigma \qquad (44)$$

Specific tension $\boldsymbol{\sigma}$ varies from about 10–100 N/cm^2 in the human muscle literature, with most studies reporting values between 25 and 40 N/cm^2. A constant value of σ is often assumed for all muscles and all subjects, although many studies have suggested σ varies between muscles and subjects and is affected by age, sex, fitness, and various other factors.

An alternative definition of PCSA was proposed by Sacks and Roy (1982):

$$PCSA_2 = (V/L_o) \cos \theta \qquad (45)$$

With this definition, the product with specific tension gives the fraction of the CC maximum isometric force that can be expressed across the tendon at pennation angle θ. Equations 43 and 45 produce identical results when θ is zero. With either definition of PCSA, the result will be inaccurate when a fiber length other than L_o is used in the denominator. Thus, values of PCSA reported from calculations involving nonnormalized fiber lengths should be interpreted with caution if they are to be used to calculate F_o. Equation 43 was used for reporting PCSA in this study because (i) it does not require knowledge of θ to calculate F_o, (ii) θ varies with muscle length and force and these factors are not controlled consistently between

studies, (iii) some implementations of the Hill model do not include fiber pennation, and (iv) some studies using Eq. 43 have not measured or reported θ, making accurate conversions impossible.

Unloaded tendon length. Measurement of $\boldsymbol{L_u}$ is complicated because the "tendon" of a muscle can be a difficult structure to define with consistency between muscles. In some muscles the tendon may run the full length of the muscle. The portion of the tendon that muscle fibers directly attach to is typically referred to as the *internal tendon* and may be fully or partially aponeurotic. The remaining portion of the tendon with no direct fiber attachments is typically referred to as the *external tendon*. The external tendon is the closest analogue to the Hill model's SEC, but some muscles have two external tendons, one distal and one proximal to the fibers. Direct assignment of L_u from measurements on tendon is therefore discouraged.

Cadaver studies can measure tendon length when the muscles have been excised from the body, assuring a truly unloaded condition. Within vivo imaging studies, it is difficult to ensure that the tendon is truly unloaded. Even in the absence of active force production, some passive force may be transmitted through the tendon.

Fiber-type distribution. Methods of defining and determining muscle fiber type vary widely and are beyond the scope of this chapter. The parameter FT is used here to represent the fraction of muscle fibers that are "fast" vs. "slow," with acknowledgement that this binary classification scheme may be overly simplistic. Readers interested in the broader spectrum of muscle fiber typing are referred to the summary by Scott et al. (2001). Readers should note that the great majority of data on muscle fiber types is expressed as the fractions of fiber numbers. Fiber types have less frequently been expressed as the fractions of cross-sectional area. This distinction is important because single "fast-twitch" fibers tend to be larger than single "slow-twitch" fibers. However, this distinction appears to only affect FT fractions by about 10% (Clarkson et al. 1980; Parkkola et al. 1993).

Parameter values. The full set of muscle parameters identified from the literature are included as a Microsoft Excel spreadsheet in the electronic supplementary material. The data are also available on bioRxiv (Miller 2016). A summary and reference list of the 29 studies from which data were obtained is included. When possible, the data were separated by sex, age, and any other relevant factors in the study such as training status. The coefficient of variation between studies, averaged over muscles and weighted by the number of samples, was 19% for L_o, 62% for θ, and 52% for PCSA. Between the four quadriceps muscles (vastus lateralis, medialis, and intermedius and rectus femoris), coefficients of variation ranged from 8 to 11% for L_o, 48–78% for θ, and 52–63% for PCSA. Coefficients of variation for L_u and FT were not calculated due to the relatively small sample sizes of those data.

Future Directions

The Hill muscle model is one of the most venerable and popular components of computer modeling in human movement science. The model is mature both in its theoretical design and its implementation on computers, but there is still room for progress in numerous areas of practical utility, including:

1. **Validation:** muscle models are typically used to estimate quantities that cannot be measured in vivo, such as muscle force, work, and energy. Direct validation of Hill model outputs is therefore challenging. Animal models provide an option for obtaining muscle forces directly for validation purposes (e.g., Lee et al. 2013), and ultrasonography provides a means for estimating in vivo human muscle force via tendon strain, which can then be compared to Hill model predictions (e.g., Dick et al. 2017).

   Indirect validation can also be a valuable approach for gaining confidence in the output of musculoskeletal models that use Hill-based muscle models. An "indirect validation" is defined here by the author as the comparison of a model-based result with an expected result from experiments on human subjects. For example, joint contact forces could be compared to data from instrumented joint replacements (Bergmann et al. 2014), or simulations of walking at different speeds or step lengths could be performed, and the model's metabolic cost could be compared to the typical U-shaped profiles seen in human experiments on metabolic cost vs. speed and step length (Bertram 2005). By verifying that the model produces accurate and expected results in such situations, the user can have greater confidence in the model's predictions for conditions that cannot be verified with human experimental data.

2. **Subject-specific parameters:** obtaining subject-specific muscle model parameters is a technically daunting and time-consuming task even for models with relatively few muscles (e.g., Hasson and Caldwell 2012). The dynamic and phenomenological nature of the model makes it unlikely that a static "scanning" procedure will ever be able to rapidly produce a set of subject-specific parameters. There is considerable knowledge still to be gained on which parameters need to be truly subject specific and how best to determine them with practical limits on cost, effort, and time investment. A promising approach is the tuning of muscle model parameters to track dynamometry data for the subjects or populations in question (e.g., Anderson et al. 2007; Hasson and Caldwell 2012). This approach carries a risk of over-fitting the model if the muscle model has too many free parameters. To avoid over-fitting, it is recommended that muscle models minimize the overall number of parameters and maximize the number of parameters with common values for all muscles (e.g., $C_{ecc}=1.5$, $v_{max}=12$) to the extent that these modeling decisions do not influence the conclusions drawn from the model's output.

   Relatedly, greater education within the field is needed on when subject-specific parameters are needed and when generic parameters can be used without compromising the validity of a study's conclusions. For example, conclusions on results from between-subject study designs could potentially depend critically on whether subject- or population-specific parameter values were used, but conclusions on results from within-subject designs are unlikely to be affected by the use of generic or generically scaled parameters even if there is uncertainty in their subject-specific values (e.g., Edwards et al. 2009). Similarly, arbitrary muscle model parameters are unlikely to affect conclusions in optimal control simulation studies where the primary outcome variables are muscle forces in data-tracking simulations (e.g., Neptune et al. 2001). As long as the parameters allow for a realistic range of forces, the

optimizer will simply adjust the muscle excitation up or down to produce the specific muscle forces needed to track the data well. However, conclusions on outcome variables involving muscle excitation, activation, work, or metabolic cost could be affected.

3. **Simulation methods:** Despite modern computational power, forward dynamics simulations with musculoskeletal models involving many Hill-based muscle model actuators still incur prohibitive computational burdens in many cases. Recent advances in modern optimal control methods such as direct collocation have greatly reduced the computational burden of such simulations with 2D models with ~10–20 muscle models (van den Bogert et al. 2011). It remains to be seen if these methods will scale well to simulations with high-dimensional 3D musculoskeletal models with ~50–100 muscle models.

4. **Muscle physiology:** the basic elements of the Hill model have been essentially unchanged since its original conception in the 1930s. Progress in experimental muscle physiology such as the discovery of titin as a potential third contractile protein could fundamentally alter our understanding of how muscles produce force (Herzog et al. 2015), with downstream implications in how best to model the phenomena of muscle force production.

References

Abbott BC, Aubert XM (1952) The force exerted by active striated muscle during and after change of length. J Physiol 117:77–86

Alexander RM, Vernon A (1975) The dimensions of knee and ankle muscles and the forces they exert. J Hum Mov Stud 1:115–123

An KN, Takahashi K, Harrigan TP, Chao EY (1984) Determination of muscle orientations and moment arms. J Biomech Eng 106:280–282

Anderson DE, Madigan ML, Nussbaum MA (2007) Maximum voluntary joint torque as a function of joint angle and angular velocity: model development and application to the lower limb. J Biomech 40:3105–3113

Bahler AS (1968) Modeling of mammalian skeletal muscle. IEEE Trans Biomed Eng 15:249–257

Bergmann G, Bender A, Graichen F, Dymke J, Rohlmann A, Trepczynski A, Heller MO, Kutzner I (2014) Standardized loads acting in knee implants. PLoS One 9:e86035

Bertram JEA (2005) Constrained optimization in human walking: cost minimization and gait plasticity. J Exp Biol 208:979–991

Buchanan TS, Lloyd DG, Manal K, Besier TF (2004) Neuromusculoskeletal modeling: estimation of muscle forces and joint moments from measurements of neural command. J Appl Biomech 20:367–395

Caldwell GE (1995) Tendon elasticity and relative length: effects on the Hill two-component muscle model. J Appl Biomech 11:1–24

Chow JW, Darling WG (1999) The maximum shortening velocity of muscle should be scaled with activation. J Appl Physiol 86:1025–1031

Clarkson PM, Kroll W, McBride TC (1980) Maximal isometric strength and fiber type composition in power and endurance athletes. Eur J Appl Physiol 44:35–42

Cole GK, van den Bogert AJ, Herzog W, Gerritsen KGM (1996) Modelling of force production in skeletal muscle undergoing stretch. J Biomech 29:1091–1104

Delp SL, Loan JP, Hoy MG, Zajac FE, Topp EL, Rosen JM (1990) An interactive graphics-based model of the lower extremity to study orthopaedic surgical procedures. IEEE Trans Biomed Eng 37:757–767

Dick TJ, Biewener AA, Wakeling JM (2017) Comparison of human gastrocnemius forces predicted by Hill-type muscle models and estimated from ultrasound images. J Exp Biol. https://doi.org/10.1242/jeb.154807

Edwards WB, Taylor D, Rudolphi TJ, Gillette JC, Derrick TR (2009) Effects of stride length and running mileage on a probabilistic stress fracture model. Med Sci Sports Exerc 41:2177–2184

Forcinito M, Epstein M, Herzog W (1998) Can a rheological muscle model predict force depression/enhancement? J Biomech 31:1093–1099

Fuglevand AJ, Winder DA, Patla AE (1993) Models of recruitment and rate coding organization in motor-unit pools. J Neurophysiol 70:2470–2488

Gordon AM, Huxley AL, Julian FJ (1966) The variation in isometric tension with sarcomere length in vertebrate muscle fibres. J Physiol 184:170–192

Günther M, Schmitt S, Wank V (2007) High-frequency oscillations as a consequence of neglected serial damping in Hill-type muscle models. Biol Cybern 97:63–79

Hasson CJ, Caldwell GE (2012) Effects of age on mechanical properties of dorsiflexor and plantarflexor muscles. Ann Biomed Eng 40:1088–1101

Hatze H (1976) The complete optimization of a human motion. Math Biosci 28:99–135

Hatze H (1977) A myocybernetic control model of skeletal muscle. Biol Cybern 25:103–119

Hatze H (1981) Estimation of myodynamic parameter values from observations on isometrically contracting muscle groups. Eur J Appl Physiol 46:325–338

He JP, Levine WS, Loeb GE (1991) Feedback gains for correcting small perturbations to standing posture. IEEE Trans Autom Control 36:322–332

Herzog W (2004) History dependence of skeletal muscle force production: implications for movement control. Hum Mov Sci 23:591–604

Herzog W, Powers K, Johnston K, Duvall M (2015) A new paradigm for muscle contraction. Front Physiol 6:174

Hicks JL, Uchida TK, Seth A, Rajagopal A, Delp SL (2015) Is my model good enough? Best practices for verification and validation of musculoskeletal models and simulations of movement. J Biomech Eng 137:020905

Hill AV (1938) The heat of shortening and the dynamic constants of muscle. Proc R Soc Lond B Biol Sci 126:136–195

Hill AV (1950) The series elastic component of muscle. Proc R Soc Lond B Biol Sci 137:273–280

Hill TL (1974) Theoretical formalism for the sliding filament model of contraction of striated muscle: part I. Prog Biophys Mol Biol 28:267–340

Huijing PA (1996) Important experimental factors for skeletal muscle modelling: non-linear changes of muscle length force characteristics as a function of degree of activity. Eur J Morphol 34:47–54

Huxley AF (1957) Muscle structure and theories of contraction. Prog Biophys Biophys Chem 7:255–318

Katz B (1939) The relation between force and speed in muscular contraction. J Physiol 96:45–64

Lee SSM, Arnold AS, de Boef MM, Biewener AA, Wakeling JM (2013) Accuracy of gastrocnemius muscles forces in walking and running goats predicted by one-element and two-element Hill-type models. J Biomech 46:2288–2295

Lichtwark GA, Wilson AM (2007) Is Achilles tendon compliance optimised for maximum muscle efficiency in locomotion? J Biomech 40:1768–1775

Lieber RL, Loren GJ, Fridén J (1994) In vivo measurement of human wrist extensor muscle sarcomere length changes. J Neurophysiol 71:874–881

Lloyd DG, Besier TF (2003) An EMG-driven musculoskeletal model to estimate muscle forces and knee joint moments in vivo. J Biomech 36:765–776

Maganaris CN, Baltzopoulos V, Sargeant AJ (1998) Changes in Achilles tendon moment arm from rest to maximum isometric plantarflexion: in vivo observations in man. J Physiol 510:977–985

McGowan CP, Neptune RR, Herzog W (2013) A phenomenological muscle model to assess history dependent effects in human movement. J Biomech 46:151–157

McLean SG, Su A, van den Bogert AJ (2003) Development and validation of a 3-D model to predict knee joint loading during dynamic movement. J Biomech Eng 125:864–874

Miller RH (2014) A comparison of muscle energy models for simulating human walking in three dimensions. J Biomech 47:1373–1381

Miller RH (2016) Summary of muscle parameters for Hill-based muscle modeling in the human lower limb. bioRxiv:090944. https://doi.org/10.1101/0909044

Minetti AE, Alexander RM (1997) A theory of metabolic costs for bipedal gaits. J Theor Biol 186:467–476

Neptune RR, Kautz SA, Zajac FE (2001) Contributions of the individual ankle plantar flexors to support, forward progression and swing initiation during walking. J Biomech 34:1387–1398

Pandy MG (1999) Moment arm of a muscle force. Exerc Sport Sci Rev 27:79–118

Parkkola R, Alanen A, Kalimo H, Lillsunde I, Komu M, Kormano M (1993) MR relaxation times and fiber type predominance of the psoas and multifidus muscle: an autopsy study. Acta Radiol 34:16–19

Riener R, Edrich T (1999) Identification of passive elastic joint moments in the lower extremities. J Biomech 32:539–544

Sacks RS, Roy RR (1982) Architecture of the hindlimb muscles of the cat: functional significance. J Morphol 173:185–195

Scott SH, Engstrom CM, Loeb GE (1993) Morphometry of human thigh muscles: determination of fascicle architecture by magnetic resonance imaging. J Anat 182:249–257

Scott W, Stevens J, Binder-Macleod SA (2001) Human skeletal muscle fiber type classifications. Phys Ther 81:1810–1816

Scovil CY, Ronsky JL (2006) Sensitivity of a Hill-based muscle model to perturbations in model parameters. J Biomech 39:2055–2063

Siebert T, Rode C, Herzog W, Till O, Blickhan R (2008) Nonlinearities make a difference: comparison of two common Hill-type models with real muscle. Biol Cybern 98:133–143

Srinivasan M (2009) Optimal speeds for walking and running, and walking on a moving walkway. Chaos 19:026112

Trotter JA (1990) Interfiber tension transmission in series-fibered muscles of the cat hindlimb. J Morphol 206:351–361

Umberger BR, Gerritsen KGM, Martin PE (2003) A model of human muscle energy expenditure. Comput Methods Biomech Biomed Engin 6:99–111

Van den Bogert AJ, Blana D, Heinrich D (2011) Implicit methods for efficient musculoskeletal simulation and optimal control. Procedia IUTAM 2:297–316

Van den Bogert AJ, Gerritsen KGM, Cole GK (1998) Human muscle modelling from a user's perspective. J Electromyogr Kinesiol 8:119–124

Van Soest AJ, Bobbert MF (1993) The contribution of muscle properties in the control of explosive movements. Biol Cybern 69:195–204

Walker SM, Schroedt GR (1974) I segment lengths and thin filament periods in skeletal muscle fibers of the rhesus monkey and the human. Anat Rec 178:63–81

Winters JM, Stark L (1985) Analysis of fundamental human movement patterns through the use of in-depth antagonistic muscle models. IEEE Trans Biomed Eng 32:826–839

Woittiez RD, Huijing PA, Rozendal RH (1983) Influence of muscle architecture on the length-force diagram of mammalian muscle. Eur J Appl Physiol 399:275–279

Zahalak GI (1981) A distribution-moment approximation for kinetic theories of muscular contraction. Math Biosci 55:89–114

Zajac FE, Gordon ME (1989) Determining muscle's force and action in multi-articular movement. Exerc Sport Sci Rev 17:187–230